

Early-Age Properties of Cement-Based Materials. I: Influence of Cement Fineness

Dale P. Bentz¹; Gaurav Sant²; and Jason Weiss³

Abstract: The influence of cement fineness on early-age properties of cement-based materials is investigated using a variety of experimental techniques. Properties that are critical to the early-age performance of these materials are tested, including heat release, temperature rise, chemical shrinkage, and autogenous deformation. Measurements of these properties for two cements of widely different fineness are supplemented with other performance measures, specifically acoustic emission measurements to listen for microcracking occurring in high performance $w/c=0.35$ mortars and dual-ring paste shrinkage measurements conducted under sealed conditions to assess residual stress development. The measured properties are observed to be quite different for the coarse and the fine cement. The current emphasis on high early-age strength within the construction industry may result in the specification of cements that are more prone to early-age cracking.

DOI: 10.1061/(ASCE)0899-1561(2008)20:7(502)

CE Database subject headings: Cements; Material properties; Aging; Experimentation.

Introduction

It is an incontrovertible fact that the finenesses of portland cements have increased during the past 50 years and are continuing to increase. Fig. 1 summarizes the mean values from three surveys as presented by the Portland Cement Association (Tennis and Bhatta 2005) and also includes individual results from the Cement and Concrete Reference Laboratory (CCRL) proficiency sample program (Cement and Concrete Reference Laboratory 2007) compiled during the past 40 years. While it can be argued that there is no guarantee that the cements selected by CCRL are representative of the cements available from the industry as a whole, taken together, all of the results in Fig. 1 clearly indicate the trend of increasing cement fineness. Both regression lines in Fig. 1 extrapolate to a typical Blaine fineness for a Type I/II cement being nearly $400 \text{ m}^2/\text{kg}$ by the year 2010. Many cements with a fineness of $400 \text{ m}^2/\text{kg}$ to $420 \text{ m}^2/\text{kg}$ are currently available. One of the main reasons for the move towards finer cements has been the ever increasing emphasis on high early-age strengths and fast track construction by much of the industry. Finer cements, with their higher surface area, are more reactive at early

ages, producing the desired higher early-age strengths. Since most cement producers are hesitant to produce a wide range of products, the same Type I/II cements that are manufactured for high early-age strength applications (high rise construction, etc.) are also employed in pavements and bridge decks, where long-term durability may be much more critical than early-age strength.

In the early 1950s, Brewer and Burrows were perhaps the first to point out the critical linkage between cement fineness and concrete durability (Brewer and Burrows 1951). This point was reiterated in the late 1960s when examining cements for use in the Dworshak Dam (Houk et al. 1969). Burrows and others have continued this advocacy for the use of coarser cements in recent years (Burrows 1998; Bentz and Haecker 1999; Burrows et al. 2004), but as Fig. 1 indicates, the trend continues much as before. The goal of this paper is to contrast a variety of early-age properties of a coarse versus a fine cement for two cements that are currently readily available on the U.S. market, to provide a quantitative data set illustrating the influences of cement fineness on early-age performance.

Experiment

Two commonly used American Society for Testing and Materials (ASTM) Type I/II portland cements that differ widely in fineness were provided from two separate cement plants of the same manufacturer. Their measured oxide compositions, projected Bogue phase compositions, specific gravities, Blaine finenesses, and measured particle size distributions (via laser diffraction) are provided in Table 1 and Fig. 2. While their chemical compositions are similar, with the exception of the coarser cement having a lower alkali content, their finenesses and particle size distributions are quite distinct. The finer cement has $25 \mu\text{m}$ as its modal value and basically contains no particles larger than $75 \mu\text{m}$, while the coarser cement has $32 \mu\text{m}$ as its modal value and contains particles up to $120 \mu\text{m}$ in diameter.

To further isolate the influence of cement fineness, all experiments on cement paste and mortar specimens were conducted at a

¹Chemical Engineer, Building and Fire Research Laboratory, National Institute of Standards and Technology, 100 Bureau Dr. Stop 8615, Gaithersburg, MD 20899 (corresponding author). E-mail: dale.bentz@nist.gov

²Ph.D. Student and Teaching Assistant, School of Civil Engineering, Purdue Univ., 550 Stadium Mall Dr., West Lafayette, IN 47907. E-mail: gsant@purdue.edu

³Professor and Assistant Head of Research, School of Civil Engineering, Purdue Univ., 550 Stadium Mall Dr., West Lafayette, IN 47907. E-mail: wjweiss@purdue.edu

Note. Associate Editor: Chiara F. Ferraris. Discussion open until December 1, 2008. Separate discussions must be submitted for individual papers. To extend the closing date by one month, a written request must be filed with the ASCE Managing Editor. The manuscript for this paper was submitted for review and possible publication on August 31, 2007; approved on November 28, 2007. This paper is part of the *Journal of Materials in Civil Engineering*, Vol. 20, No. 7, July 1, 2008. ©ASCE, ISSN 0899-1561/2008/7-502-508/\$25.00.

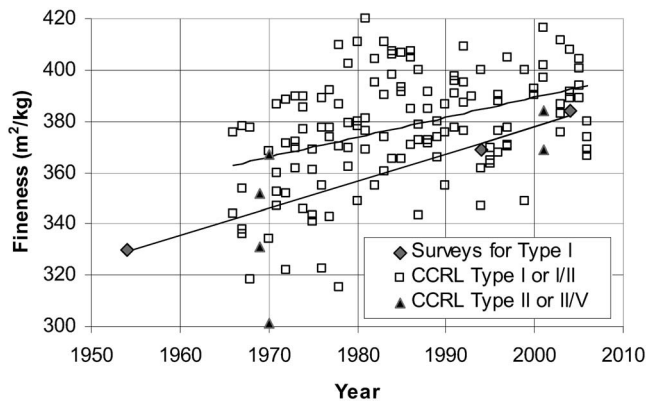


Fig. 1. Changes in the Blaine fineness of cements from the 1950s to the present day. Regression lines are provided for the Type I survey and CCRL Type I or I/II data sets only.

single value of water-to-cement ratio (w/c) of 0.35 by mass. This w/c was selected to be low enough to avoid any issues with bleeding and settlement of the cement particles, while still being in the range of values often utilized in concretes for high performance and paving applications. In general, cement paste and mortar mixtures were prepared without any chemical admixtures, as the purpose of this study is to focus on cement performance. However, to enable proper placement and enhance workability, a low dosage of a water-reducing admixture was used in preparation of the mortar mixtures and cement pastes evaluated for acoustic emission and restrained shrinkage performance, respectively. The water content of the admixture was accounted for in proportioning these mixtures. For measurements of calorimetry, chemical shrinkage, and setting time, cement pastes with no chemical admixtures were prepared using a high shear blender, while mortars (strength, deformation, and acoustic emission) were prepared according to the ASTM C305-99 procedures (ASTM 1999a). The mortar mixture proportions are provided in Table 2. The two different mortar proportions were prepared at two different laboratories, with each employing their preferred mixture de-

Table 1. Cement Oxide Compositions, Bogue Potential Phase Mass Fractions, and Fineness

Oxide or property	Fine cement	Coarse cement
CaO	0.633	0.648
SiO ₂	0.203	0.209
Al ₂ O ₃	0.045	0.045
Fe ₂ O ₃	0.0339	0.041
SO ₃	0.0268	0.022
Na ₂ O	0.00077	0.003 (equivalent)
K ₂ O	0.00622	Not reported
MgO	0.0373	0.012
P ₂ O ₅	0.00127	Not reported
TiO ₂	0.00309	Not reported
Bogue—C ₄ AF	0.103	0.125
Bogue—C ₃ A	0.062	0.050
Bogue—C ₃ S	0.625	0.625
Bogue—C ₂ S	0.109	0.127
Specific gravity	3.22	3.21
Fineness (Blaine)	380 m ² /kg	311 m ² /kg
Median particle diameter	11.5 μm	17 μm

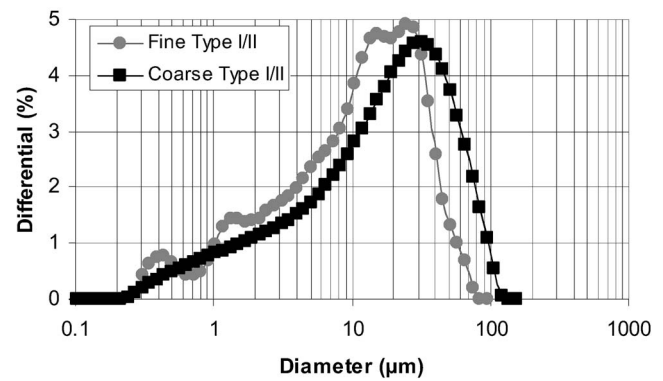


Fig. 2. Measured differential particle size distributions for the two cements

sign. For measurements of restrained shrinkage (dual-ring tests), deaired neat cement pastes with a water reducer (0.5% by mass of cement) were prepared according to the procedure specified in Sant et al. (2006). Pastes, as opposed to mortars, were selected for the ring tests to maximize the cracking potential, due to their increased shrinkage relative to mortars.

The following measurements were conducted on the cement paste and mortar specimens:

1. Isothermal calorimetry—the heat of hydration was measured during the course of 7 d on 5.25 g samples of premixed cement pastes using a TAM air calorimeter (certain commercial products are identified in this paper to specify the materials used and procedures employed. In no case does such identification imply endorsement by the National Institute of Standards and Technology, nor does it indicate that the products are necessarily the best available for the purpose); to provide an indication of variability, two specimens from the same batch of paste were evaluated in neighboring cells of the calorimeter for each cement.
2. Semiadiabatic calorimetry—the semiadiabatic temperature rise was measured during the course of 3 d on single cement paste specimens with a mass of approximately 330 g using a custom-built semiadiabatic calorimeter unit (Bentz and Turpin 2007); replicate specimens from individual batches with the same mixture proportions have indicated a standard deviation of 1.4°C in the maximum specimen temperature achieved during a 3 d test.
3. Chemical shrinkage—measured during the course of 8 d or 12 d on triplicate $w/c=0.35$ cement paste specimens pre-

Table 2. Mortar Mixture Proportions Used in the Study

Material	Mixture proportions (strength and autogenous deformation)	Mixture proportions (acoustic emission)
Type I/II cement	1,000.0 g	1,000.0 g
Water	350.0 g	350.0 g
F95 fine sand ^a	522.5 g	—
Graded sand (ASTM C 778 ^b)	397.1 g	1,750.0 g
20–30 sand (ASTM C 778)	397.1 g	—
GS16 coarse sand ^a	773.3 g	—
Water reducer	—	5.30 g

^aF95 and GS16 correspond to sand supplier designations.

^bASTM 2005a.

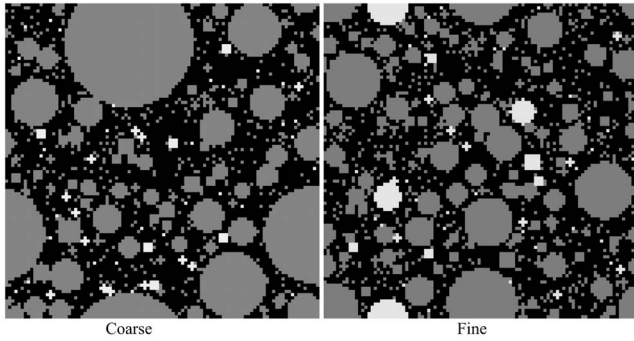


Fig. 3. Single two-dimensional slice images (100 μm by 100 μm) from three-dimensional simulated starting microstructures for $w/c=0.35$ cement pastes for the cements of two different finenesses (cement particles are gray and gypsum particles are white)

pared from a single batch, using the ASTM C 1608 standard test method (ASTM 2005b); according to the ASTM standard, the expected precision for the test is 0.0042 kg of water per kg of cement.

4. Time of setting—measured on single cement paste specimens based on penetration of the Vicat needle according to ASTM C 191 (ASTM 1999b); in the standard, the single laboratory precisions are listed as 12 min and 20 min for initial and final time of setting, respectively.
5. Compressive strength—measured at 1 d, 3 d, 7 d, and 28 d on $w/c=0.35$ mortar cube specimens, according to the procedures in ASTM C 109 (ASTM 1999c), but with a loading rate of 20.7 MPa/min, switching to deformation control once a stress of 13.8 MPa was reached; three specimens from a single batch of mortar were evaluated at each time, with the averages and standard deviations being provided in the results to follow.
6. Autogenous deformation—measured on duplicate mortar specimens prepared from the same batch, sealed in corrugated tubes (Jensen and Hansen 1995) (procedure is currently being standardized in ASTM subcommittee C09.68); in the draft standard, the single laboratory precision is listed as 30 microstrains for mortar specimens.
7. Restrained shrinkage tests—measured on single specimens of each cement paste using a dual-ring configuration, with the specimens sealed for 5 d (Weiss et al. 2006; Sant et al. 2007); in ASTM C 1581 (ASTM 2004b), the single laboratory repeatability standard deviation of the age at cracking is listed as 2 d.
8. Acoustic emission—measured on duplicate sealed mortar specimens prepared from the same batch, using procedures described in detail previously (Kim and Weiss 2003; Charriton and Weiss 2002).

At a constant w/c ratio, the initial three-dimensional microstructures based on these two cements will be vastly different. To illustrate this point, Fig. 3 shows two-dimensional images from simulated three-dimensional starting microstructures (Bentz 1997) where the assumed spherical cement particle diameters follow the two distributions provided in Fig. 2. Each two-dimensional image is 100 μm by 100 μm . Clearly, the interparticle spacing (initial pore size) is much greater in the microstructure based on the coarser of the two cements. This interparticle spacing will have a large influence on the development of autogenous stresses and strains within the hydrating cement paste and mortar specimens (Bentz et al. 2001). In addition,

Table 3. Compressive Strength Results for $w/c=0.35$ Mortar Cubes

Age	Compressive strength—fine (MPa)	Compressive strength—coarse (MPa)
1 d	36.2 (1.4) ^a	18.5 (1.2)
3 d	55.6 (2.4)	35.8 (3.1)
7 d	64.8 (1.0)	44.4 (2.4)
28 d	78.5 (2.2)	58.0 (3.5)

^aNumbers in parentheses indicate one standard deviation as determined for the three replicate specimens tested at each age.

the much larger surface area presented by the finer cement (Fig. 3) should result in increased rates of hydration and internal energy (heat of hydration) production.

Results and Discussion

Compressive Strength

First, the compressive strength results are considered to provide a frame of reference in which to consider the other early-age property measurements. As shown in Table 3, the finer cement consistently produces higher compressive strengths at all four testing ages. These increased compressive strengths at any given age are likely due to a combination of their increased reactivity and the smaller interparticle spacing exhibited in Fig. 3. At an age of 1 d, the coarser cement achieves only about 50% of the compressive strength of the finer one. By 28 d, however, it achieves 74% of the strength exhibited by its finer counterpart. This exemplifies the general movement towards higher early-age strengths as the finer cement mortar achieves almost 50% of its 28 d strength after just 1 d and over 70% of its 28 d strength in just 3 d. For the coarser cement mortar, these corresponding values are only 32 and 62%, respectively. And of course, a 28 d mortar cube compressive strength of 58 MPa, as exhibited by the coarser cement, would be sufficient for many construction applications.

Calorimetry

Two major contributions to early-age cracking of cement-based materials are thermal and autogenous stresses and deformations (ACI 2008). While the magnitudes of thermal stresses and strains will be highly influenced by the heat transfer conditions between the curing concrete and its environment, one key concrete material property is the energy generated within the concrete element due to the exothermic cement hydration reactions. Both isothermal and semiadiabatic calorimetry can be used to provide valuable insights into these reactions. Isothermal calorimetry provides a measure of the reaction rate (heat released) at a constant temperature, while semiadiabatic calorimetry provides a closer representation of actual field conditions where a portion of the energy released by the reactions will raise the temperature of the concrete, further increasing the reaction rates in an autocatalytic manner. It would generally be expected that a finer cement will have an increased heat release rate (Bentz et al. 1999) and a corresponding larger temperature rise in a semiadiabatic experiment, although the ultimate heat releases may be similar.

Isothermal calorimetry results for specimens tested at 25°C for the two cements are provided in Fig. 4. ASTM C 150 (ASTM 2007) specification limits on the 7 d heat of hydration for Type II (optional limit) and Type IV cements are also indicated in the figure. The coarser cement is seen to meet (falling below) the

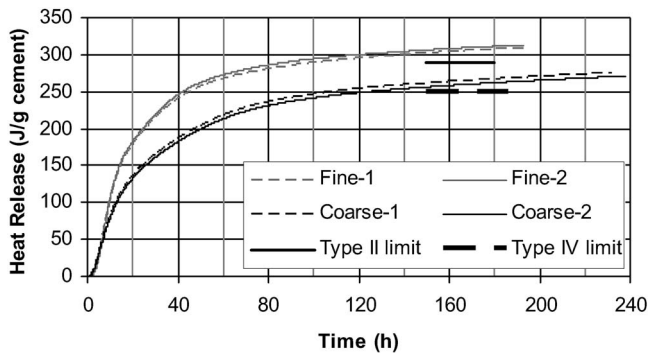


Fig. 4. Isothermal calorimetry at 25°C for replicate specimens of $w/c=0.35$ pastes

optional limit of 290 J/g cement for the 7 d heat of hydration for a Type II cement (selected for general use, especially when a moderate sulfate resistance or moderate heat of hydration is desired), while neither cement could be classified as a Type IV cement (selected for use when a low heat of hydration is desired) based on heat of hydration, as both exceed the Type IV 7 d limit of 250 J/g cement. This is to be expected, as to the best of the authors' knowledge, few if any Type IV cements are currently produced in the United States. In Fig. 4, the variability between the two replicate specimens of each cement is seen to be minimal. Isothermal calorimetry experiments were also conducted at 10°C and 40°C to determine apparent activation energies for the two cements. For the finer cement, an activation energy of 37 kJ/mol was determined; the corresponding value for the coarser cement was 38 kJ/mol. Both of these are close to the value of 40 kJ/mol recommended as the default value by the ASTM C 1074 standard (ASTM 2004a). The higher heat release rate of the finer cement will generally lead to larger temperature rises within and larger temperature gradients through concrete elements, both of which can increase the risk of early-age cracking (ACI 2008).

This increased temperature rise is further exemplified by Fig. 5 that shows the semiadiabatic temperature rise versus time for equivalent cement pastes prepared with the two cements of different fineness. Initially, the temperature rise is fairly similar, but after about 5 h, the higher reaction rate of the finer cement results in an increased temperature rise (that further accelerates the cement hydration reactions). Eventually, much of the cement has reacted, such that the temperature rise cannot be maintained and the heat losses to the environment in the semiadiabatic experimental configuration begin to dominate over the heat produced by the hydration reactions. Thus, after the peak temperature is

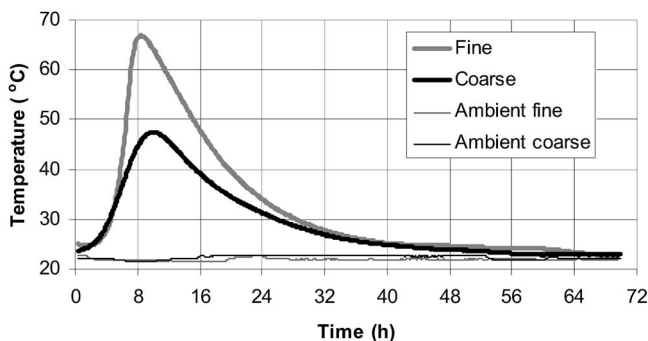


Fig. 5. Semiadiabatic temperature rise for $w/c=0.35$ cement pastes

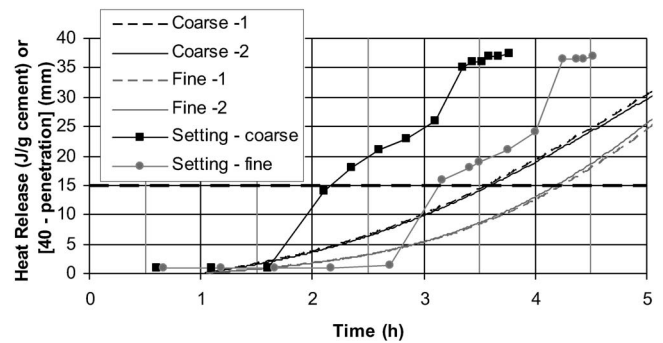


Fig. 6. Vicat setting (plotted as 40—needle penetration) and heat release for $w/c=0.35$ cement pastes—initial set (ASTM C191) (ASTM 1999b) is indicated by the heavy dashed line

reached (with a peak rise of about 40°C after 8 h for the finer cement and a peak rise of about 25°C after 10 h for the coarser cement), the temperature gradually returns to ambient. In terms of thermal cracking, it is not only the maximum peak temperature achieved, but also the rate of this subsequent decrease that can contribute to early-age cracking (ACI 2008). Furthermore, as the specimen temperature exceeds 60°C, hydration products such as (primary) ettringite may become unstable; then, the later precipitation of secondary ettringite some time after subsequent cooling may present a serious durability concern (Day 1992). For many concrete elements in many field environments, the “relatively extreme” temperature rises seen in Fig. 5 would not be reproduced due to greater heat transfer between the concrete and the environment. However, for large (mass) concrete structures, the temperature rises could be even more severe than those shown in Fig. 5. For this reason, heat release has always been a major concern in dams and other large concrete structures (Houk et al. 1969). In addition to coarser cements, other mitigation techniques such as the addition of slower reacting pozzolans, chilled aggregates, ice additions as part of the mixing water, and the use of cooling pipes have been employed (ACI 1999, 2005).

Setting Characteristics

The setting characteristics of the cement pastes were characterized based on Vicat needle penetration measurements. The results are presented in Fig. 6, along with the early-age isothermal calorimetry curves. Rather surprisingly, the coarser cement exhibits an earlier setting time as it exhibits an early-age reactivity that is greater than that of the finer cement, as illustrated by the heat release curve in Fig. 6. The two heat of hydration curves later cross one another at 7 h and beyond that point; as shown in Fig. 4, the finer cement proceeds to release more heat than the coarser one. Considering that the degree of hydration should be proportional to heat release (Bentz 1997), a careful examination of Fig. 6 also reveals that the coarser cement is requiring slightly less hydration to achieve equivalent “set” (Vicat needle penetration) than the finer cement, in agreement with previous predictions based on three-dimensional microstructure modeling (Bentz et al. 1999).

Chemical Shrinkage

Another measure of early-age hydration rates can be provided by chemical shrinkage measurements (ASTM 2005b; Powers 1935; Geiker and Knudsen 1982). While the ASTM test method speci-

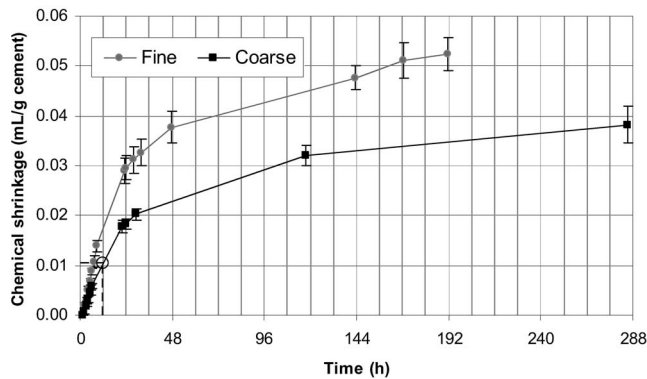


Fig. 7. Chemical shrinkage at 25°C for $w/c=0.35$ cement pastes. Error bars represent one standard deviation determined based on three replicate specimens for each cement—dashed lines and large empty circle indicate the 12-h limit (0.0105 mL/g cement) set by Burrows et al. (2004) for a low crack cement

fies a w/c ratio of 0.4 in order to minimize both bleeding and depercolation effects (ASTM 2005b), here measurements were performed on pastes with $w/c=0.35$ to be consistent with the other measurements performed in this study. The results, provided in Fig. 7, once again indicate the enhanced reactivity of the finer cement relative to the coarser one. It is quite interesting to also note that the coarser cement just meets the requirement of having a 12 h chemical shrinkage less than or equal to 0.0105 mL/g cement, as suggested previously for producing a crack resistant cement (Burrows et al. 2004).

In Fig. 8, it is demonstrated that the hydration rates as measured by chemical shrinkage or heat of hydration for these two particular cements are equivalent when using a scaling factor. In 1935, Powers determined this scaling factor to convert from chemical shrinkage to heat release to be 80.8 (J/g)/(g water/100 g cement), for four different cements of that era (Powers 1935). More recently (Bentz 1997), scaling factors of 70.7 (J/g)/(g water/100 g cement) and 86.2 (J/g)/(g water/100 g cement) have been determined for CCRL proficiency cements 115 and 116 (Cement and Concrete Reference Laboratory 2007), respectively. For the results presented in Fig. 8, the scaling factors are 66.5 (J/g)/(g water/100 g cement) and 77.8 (J/g)/(g water/100 g cement) for the finer and coarser cements, respectively, in reasonable agreement with the previously determined values. This scaling factor

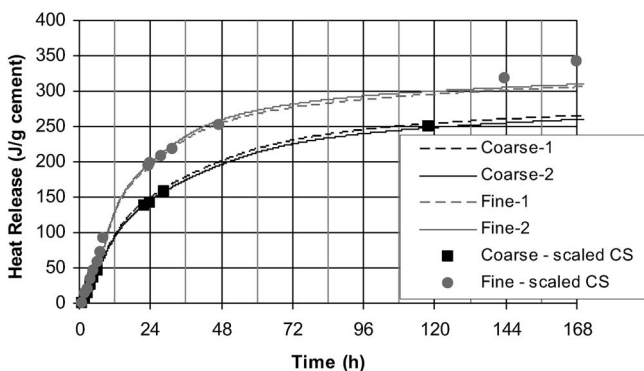


Fig. 8. Scaled chemical shrinkage (CS) along with heat of hydration for the two cements—scaling factors utilized for chemical shrinkage are provided in the text

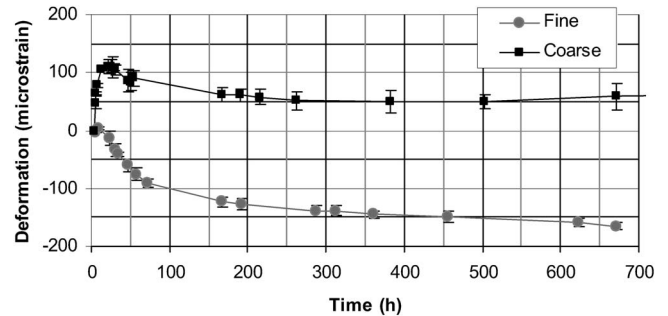


Fig. 9. Autogenous deformation of $w/c=0.35$ mortars cured under sealed conditions at 25°C—error bars represent one standard deviation determined based on two replicate specimens for each mortar

will be a function of cement phase composition and individual phase reactivities, as each phase has unique heats of hydration (Bentz 1997) and chemical shrinkages (Powers 1935) per unit mass.

Autogenous Deformation

In addition to providing a convenient measure of early-age hydration rates, chemical shrinkage measurements also provide an indication of the volume of empty porosity that will be created in a cement-based material cured under sealed conditions. As such, it is one of the key determinations in properly proportioning a concrete mixture to incorporate internal curing, for example (Bentz et al. 2005). The results in Fig. 7 would indicate that the creation of empty porosity, namely, self-desiccation, will be more severe at early ages in the finer cement paste. In addition to the volume of empty porosity being created, the sizes of the pores being emptied (according to the Kelvin-Laplace equation) also greatly influences the development of autogenous stresses and strains in these materials (Bentz et al. 2001). Fig. 3 would suggest that smaller pores will be emptied in the finer cement systems. With both an enhanced self-desiccation and the emptying of smaller pores, the autogenous shrinkage of a mortar made with the finer cement should be much greater than that of one containing the coarser cement.

As shown in Fig. 9, this is indeed the case. In fact, the coarser cement mortar actually exhibits a net autogenous expansion at 28 d, as has been observed previously for $w/c=0.35$ cement pastes based on cements with Blaine finenesses of 212 m^2/kg and 254 m^2/kg (Bentz et al. 2001). In that study, cement pastes made using cements with Blaine finenesses of 387 m^2/kg and 643 m^2/kg both exhibited autogenous shrinkages of more than -500 microstrains. The microstrains measured for the mortar based on the finer cement in this study are lower than this due to the dilution factor (less shrinking cement paste per unit volume in a mortar versus a paste), the internal restraint offered by the sand particles, and possibly a reduction in autogenous stresses resulting from the presence of larger pores in the interfacial transition zones between cement paste and sand particles (Bentz et al. 1999; Pease et al. 2003).

The exact cause of the expansion in the case of the coarser cement is unknown, but it is commonly conjectured to be due to either ettringite formation or local water imbibition and swelling of the cement hydration products (Bentz et al. 2001). This same expansion would be present in the finer cement system, but, in that case, would simply be overwhelmed by the autogenous shrinkage. Thus, the autogenous deformation plotted in Fig. 9 is

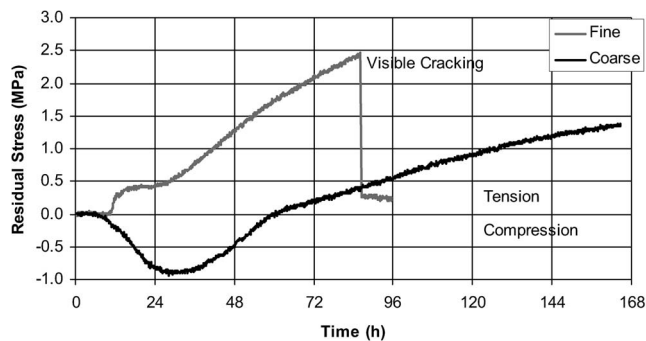


Fig. 10. Residual stress development as a function of time for $w/c = 0.35$ coarse and fine cement pastes cured under sealed conditions at 23°C

the sum of (at least) two competing effects and which one dominates depends not only on the cement fineness (Bentz et al. 2001), but also on the w/c ratio (Baroghel-Bouny et al. 2006; Bentz et al. 2008). For each cement having a given degree of fineness, there will be a critical w/c below which the measured autogenous deformation will exhibit a net shrinkage and above which a net expansion will be measured (Baroghel-Bouny et al. 2006; Bentz et al. 2008).

Restrained Ring Shrinkage Testing

Fig. 10 shows residual stress development in coarse and fine cement pastes assessed using a dual ring, restrained shrinkage test. As seen in the figure, the fine cement shows no stress development until 11 h after which time the measured residual stresses begin to increase. This is similar to the evolution of free shrinkage experienced by the specimen over this time (Fig. 9). A peak residual stress (tensile) of 2.45 MPa develops in the ring specimen at 87 h, and a visible crack appears, as the residual stress developed has exceeded the strength (tensile) of the specimen. The coarse cement specimen shows no development of residual stresses, until 6.5 h, after which time a compressive stress begins to develop in the specimen. This is in agreement with the earlier set time (Fig. 6), and autogenous expansion measured for this cement (Fig. 9). A peak compressive stress of 0.9 MPa is observed to develop in this specimen at 29 h. After this time, the magnitude of the compressive stress developed is observed to consistently decrease, until an age of 61 h, when the development of net tensile stresses initiates in the specimen. A peak tensile stress of 1.4 MPa develops in the coarse cement mortar at a specimen age of 165 h, when the test was terminated due to equipment availability limitations. No cracking was observed in the coarse cement system during the course of the test. Consequently, even though coarse cements develop a lower strength as compared to fine cements (Table 3), coarse cement systems may exhibit a decreased risk of cracking at early ages, due to their decreased autogenous shrinkage.

Acoustic Emission

To quantify damage development (microcracking) in the cement mortars, the acoustic energy release was recorded. Acoustic energy is defined as the cumulative area under the voltage versus time response for each acoustic event; and provides quantifiable information that can be related to the mechanical fracture energy of cementitious composites (Landis and Ballion 2002). The

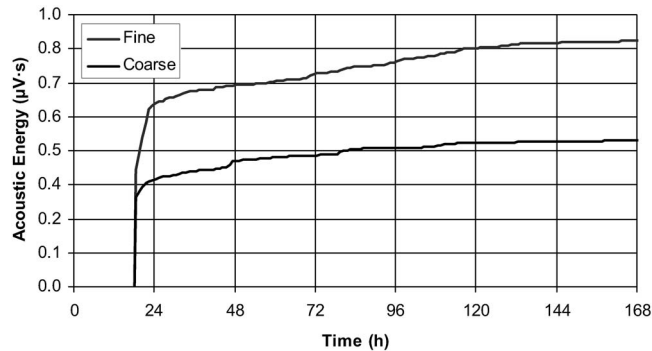


Fig. 11. Cumulative acoustic energy as a function of time for $w/c = 0.35$ coarse and fine cement mortars cured under sealed conditions at 23°C

acoustic emission sensors are piezoelectric transducers that convert a “sensed” vibration/disturbance (acoustic event) into an electrical signal. This is measured in terms of an energy unit by the data acquisition interface. This energy unit is then converted and expressed in terms of microvolt seconds ($\mu\text{V}\cdot\text{s}$) and corresponds to the absolute value of the cumulative area under the voltage versus time graph. Fig. 11 shows the cumulative acoustic energy measured for the coarse and fine cement mortars. Soon after the time of initiation of the test (at 18 h), a rapid increase (and divergence) in acoustic energy is observed in the fine cement mortar. After this time, the acoustic energy recorded in the fine and coarse mortar is observed to increase, although at a higher rate for the fine cement system. In addition, the acoustic energy released by the fine cement mortar is observed to be consistently higher than that of the coarse cement mortar. This can be explained by the higher autogenous shrinkage experienced by the fine mortar (Fig. 9), which would promote microcracking at the paste-aggregate interfaces at very early ages (<24 h) (Chariton et al. 2002). These results would indicate lower damage development and less expended fracture energy in coarse cement systems, which would contribute to a lower risk of early-age cracking.

Conclusions

Comprehensive studies of a variety of early-age properties of coarse and fine cement pastes and mortars have been conducted including compressive strength, isothermal calorimetry, semiadiabatic temperature rise, setting time, chemical shrinkage, autogenous deformation, restrained ring shrinkage, and acoustic emission. These studies have indicated that:

- Chemical shrinkage and heat of hydration are both valid indicators of early-age hydration.
- While the coarser cement exhibits compressive strengths well below those of the finer cement at all ages tested, it also releases less heat and results in a substantially lower semiadiabatic temperature rise.
- The coarse cement system initially develops a compressive stress, exhibiting lower residual stress development and a lower risk of cracking at early ages as compared to the fine cement system. This is primarily due to a lower magnitude of autogenous deformation experienced by these (coarse cement) systems, contributing to a decrease in autogenous stresses developed in coarse cement systems.
- As exemplified by the results of this study, high early-age

strength cements will generally increase both the thermal and autogenous deformation contributions to early-age cracking.

Acknowledgments

The writers would like to thank the Lehigh Portland Cement Co. for providing the two cements used in this study.

References

- American Concrete Institute (ACI). (1999). "Hot weather concreting." *ACI 305R-99*, Farmington Hills, Mich.
- American Concrete Institute (ACI). (2005). "Guide to mass concrete." *ACI 207.1R-05*, Farmington Hills, Mich.
- American Concrete Institute (ACI). (2008). "Early-age cracking: Causes, measurements, and mitigation." *State-of-the-Art Rep. of ACI Committee 231*.
- ASTM. (1999a). "Standard practice for mechanical mixing of hydraulic cement pastes and mortars of plastic consistency." *C 305-99*, West Conshohocken, Pa.
- ASTM. (1999b). "Standard test method for time of setting of hydraulic cement by Vicat Needle." *C 191-99*, West Conshohocken, Pa.
- ASTM. (1999c). "Standard test method for compressive strength of hydraulic cement mortars (using 2 in. or [50 mm] cube specimens)." *C 109/C, 109M-99*, West Conshohocken, Pa.
- ASTM. (2004a). "Standard practice for estimating concrete strength by the maturity method." *C 1074-04*, West Conshohocken, Pa.
- ASTM. (2004b). "Standard test method for determining age at cracking and induced tensile stress characteristics of mortar and concrete under restrained shrinkage." *C 1581-04*, West Conshohocken, Pa.
- ASTM. (2005a). "Standard specification for standard sand." *C 778-05*, West Conshohocken, Pa.
- ASTM. (2005b). "Standard test method for chemical shrinkage of hydraulic cement paste." *C 1608-05*, West Conshohocken, Pa.
- ASTM. (2007). "Standard specification for portland cement." *C 150-07*, West Conshohocken, Pa.
- Baroghel-Bouny, V., Mounanga, P., Khelidj, A., Loukili, A., and Rafai, N. (2006). "Autogenous deformation of cement pastes. Part II. W/C effects, micro-macro correlations, and threshold values." *Cem. Concr. Res.*, 36, 123–136.
- Bentz, D. P. (1997). "Three-dimensional computer simulation of cement hydration and microstructure development." *J. Am. Ceram. Soc.*, 80(1), 3–21.
- Bentz, D. P., Garboczi, E. J., Haecker, C. J., and Jensen, O. M. (1999). "Effects of cement particle size distribution on performance properties of portland cement-based materials." *Cem. Concr. Res.*, 29, 1663–1671.
- Bentz, D. P., and Haecker, C. J. (1999). "An argument for using coarse cements in high performance concretes." *Cem. Concr. Res.*, 29(4), 615–618.
- Bentz, D. P., Jensen, O. M., Hansen, K. K., Olesen, J. F., Stang, H., and Haecker, C. J. (2001). "Influence of cement particle-size distribution on early age autogenous strains and stresses in cement-based materials." *J. Am. Ceram. Soc.*, 84(1), 129–135.
- Bentz, D. P., Lura, P., and Roberts, J. W. (2005). "Mixture proportioning for internal curing." *Concr. Int.*, 27(2), 35–40.
- Bentz, D. P., Peltz, M., and Winpiger, J. (2008). "Early-age properties of cement-based materials: II. Influence of water-to-cement ratio." *J. Mater. Civ. Eng.*, in review.
- Bentz, D. P., and Turpin, R. (2007). "Potential applications of phase change materials in concrete technology." *Cem. Concr. Compos.*, 29(7), 527–532.
- Brewer, H. W., and Burrows, R. W. (1951). "Coarse-ground cement makes more durable concrete." *J. Am. Concr. Inst.*, 22(5), 353–360.
- Burrows, R. W. (1998). "The visible and invisible cracking of concrete." *Monograph No. 11*, American Concrete Institute, Farmington Hills, Mich.
- Burrows, R. W., Kepler, W. F., Hurcomb, D., Schaffer, J., and Sellers, G. (2004). "Three simple tests for selecting low-crack cement." *Cem. Concr. Compos.*, 26(5), 509–519.
- Cement and Concrete Reference Laboratory. (2007). (<http://www.ccril.us>) (June 2007).
- Chariton, T., Kim, B., and Weiss, W. J. (2002). "Using passive acoustic energy to quantify cracking in volumetrically restrained cementitious systems." *Proc., 15th EMD Conf.* (CD-ROM), ASCE, Reston, Va.
- Chariton, T., and Weiss, W. J. (2002). "Using acoustic emission to monitor damage development in mortars restrained from volumetric changes." *Proc., Concrete: Material Science to Application, A Tribute to Surendra P. Shah*, P. Balaguru, A. Namaan, and W. J. Weiss, eds., ACI SP-206, 205–218.
- Day, R. L. (1992). "The effect of secondary ettringite formation on the durability of concrete: A literature analysis." *Rep. No. RD108*, Portland Cement Association, Skokie, Ill.
- Geiker, M., and Knudsen, T. (1982). "Chemical shrinkage of portland cement pastes." *Cem. Concr. Res.*, 12, 603–610.
- Houk, I. E., Jr., Borge, O. E., and Houghton, D. R. (1969). "Studies of autogenous volume change in concrete for Dworshak Dam." *ACI J.*, 66(45), 560–568.
- Jensen, O. M., and Hansen, P. F. (1995). "A dilatometer for measuring autogenous deformation in hardening portland cement paste." *Mater. Struct.*, 28, 406–409.
- Kim, B., and Weiss, W. J. (2003). "Using acoustic emission to quantify damage in restrained fiber reinforced cement mortars." *Cem. Concr. Res.*, 33(2), 207–214.
- Landis, E., and Ballion, L. (2002). "Experiments to relate acoustic energy to fracture energy of concrete." *J. Eng. Mech.*, 128(6), 698–702.
- Pease, B., Neuwald, A., and Weiss, W. J. (2003). "The influence of cement fineness on early age shrinkage in fresh cementitious systems." *Proc., Celebrating Concrete*, 329–338.
- Powers, T. C. (1935). "Adsorption of water by portland cement paste during the hardening process." *Ind. Eng. Chem.*, 27, 790–794.
- Sant, G., Lura, P., and Weiss, W. J. (2006). "Measurement of volume change in cementitious materials at early ages: Review of testing protocols and interpretation of results." *Transportation Research Record. 1979*, Transportation Research Board, Washington, D.C.
- Sant, G., Rajabipour, F., Lura, P., and Weiss, W. J. (2007). "Examining residual stress development in cementitious materials experiencing an early-age expansion." *Proc., 9th CANMET-ACI Int. Conf.—T.C. Holland Symp.*, 21–29.
- Tennis, P. D., and Bhaty, J. I. (2005). "Portland cement characteristics—2004." *Concr. Tech. Today*, 26(3), 1–3.
- Weiss, J., Lura, P., Rajabipour, F., and Sant, G. (2006). "Performance of shrinkage reducing admixtures at different humidities and at early ages." *ACI Mater. J.*, accepted for publication.